Unified Analysis of Switched-Capacitor Resonant Converters

Y. P. Benny Yeung, K. W. E. Cheng, *Member, IEEE*, S. L. Ho, K. K. Law, and Danny Sutanto, *Senior Member, IEEE*

***Abstract*—A family of switched-capacitor resonant circuits using only two transistors is presented. The circuit operates under zero-current switching and, therefore, the switching loss is zero. It also offers a wide choice of voltage conversions including fractional as well as multiple and inverted voltage conversion ratios.**

***Index Terms*—DC/DC power conversion, resonant power conversion, switched-capacitor circuits, switched circuits, switched-mode power supplies.**

I. Introduction

THE classical switched-mode converter has been a popular topology for dc/dc power conversion because it is technologically mature and is easy to use. One of the main disadvantages is that the size of their energy storage components, namely, capacitor and inductor, are very dependent on the switching frequency. Hence, the power density of the converter is limited. Soft-switching converters [1], [2] allow the switching devices to operate under zero-current/voltage switching, therefore, the switching loss is small and high switching frequency is possible. However, the size of the filter, resonant inductors, and resonant capacitors dominate the overall size of the converter. For a practical engineer, the design of an inductor is critical to the whole converter. In fact, the inductor is typically the largest component in a converter.

Switched-capacitor converters [3] do not require any inductor. Therefore, much research has been carried out to develop such inverters during the last decade or so. Usually, these converters require a large number of transistors to change the topology of the circuit by connecting a switching capacitor between the source and load [4], [5]. The voltage regulation of such converter is also difficult because the magnitude of the output voltage must be a fraction or a multiple of the source voltage [6], [7]. In order to regulate the converter, the switching capacitor's charge and discharge characteristics must also be taken into account and, thus, the switching device's duty ratio is used to control the amount of power through the switching capacitor. The drawback of this converter is that the transistor's on-state resistance and the equivalent series resistance of the capacitor must have the same order of magnitude as the capacitor's impedance. Such constraint would decrease the efficiency of the converter. Indeed, this principle is also analogous to that of the outdated linear resistive power supply. Research works on the switching capacitor are, however, progressing at a phenomenal rate. The topology variation [8] also shows the usual work on the analysis of the high-order operation of the converter.

One of the major drawbacks of the prior art is the nonzero-current switching of the switching capacitor. Current spike exists on all these prior art circuit components and its peak value is especially high because of the "short circuiting" of two voltages when the switching capacitor is connected among the source voltage, output voltage, and other capacitors in the circuits. This is because the basic principle of the converter is to charge a switching capacitor from the input source and connect it to the output load. The switching capacitor is exposed to a potential difference between the source/load and the switching capacitor and results in a high current spike which is only limited by the parasitic inductance in the circuit. This current spike is uncontrollable and it generates extra electromagnetic interference (EMI) and switching loss. This is one of the main reasons that the conventional switched-capacitor converters are only limited to small ratings, typically, a couple of tens of watts [3]–[8]. In order to rectify this inherent problem of the switched-capacitor converter and to make the current controllable and also to have zero-current switching, a resonance feature is added to the converter in the proposed topology. In other words, this paper presents a concept which combines the resonant converters [9] and switched-capacitor converters, referred to as a switched-capacitor resonant converter which combines all the favorite features of the two methods. A very small inductor is added to create a resonant turn-on and turn-off when the transistors are switched on or off, respectively. Zero-current switching condition in both switching on and off is obtained so that both switched loss and electromagnetic interference are low. Transistor current is limited by the small resonant inductor and, hence, the current spike problem of switched-capacitor can be solved. Thus, the power level of the proposed circuit is higher than conventional switched-capacitor converters. Comparisons between conventional dc–dc converters, conventional switched-capacitor converters, and the proposed switched-capacitor resonant converters are shown in Table I. By the features of the proposed converters, the converters can be used as a post-regulator of dc–dc converters and power-factor-correction converters. It can also be applied to portable electronic equipment and any low-profile equipment like notebook computers and portable digital assistants (PDAs). A preliminary study of this converter has been presented in

Manuscript received October 5, 2001; revised November 18, 2003. Abstract published on the Internet May 20, 2004. This work was supported by the Research Committee of The Hong Kong Polytechnic University and the Research Grants Council of Hong Kong under Project PolyU5085/98E.

The authors are with the Department of Electrical Engineering, The Hong Kong Polytechnic University, Hong Kong (e-mail: eeecheng@polyu.edu.hk).

Digital Object Identifier 10.1109/TIE.2004.831743

TABLE I
COMPARISON OF CONVENTIONAL CONVERTERS AND PROPOSED CONVERTERS

	Conventional DC-DC Converter	Conventional Switched- capacitor Converter	Proposed Switched- capacitor Resonant Converter
Magnetic Components	Large inductor or transformers is needed.	No magnetic component is needed.	Very small inductor is needed. Normally air-core inductor is used.
Current Stress	Low	Very high	Low
Amount of Transistors	Few transistors are needed.	Number of transistors depended on fractional or multiple ratios of output voltage and input voltage. High fractional or multiple ratio leads to large amount of transistors needed.	Two transistors are needed in all fractional or multiple ratio of output voltage and input voltage.
Fabrication Flexibility	Cannot be fabricated in integrated chips.	Able to be fabricated in integrated chips.	Able to be fabricated in integrated chips.
Height	Normally high. Special low profile magnetic component is needed if low profile shape of converter is required.	Low	Low
Power Level	Low to high	Low	Low to medium
Efficiency	High	Low	High

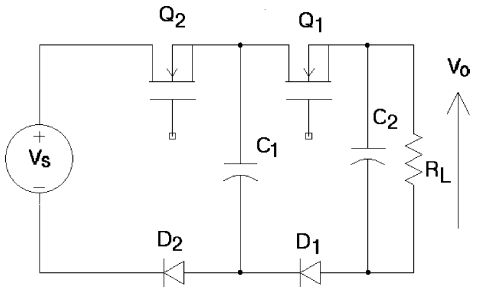

Fig. 1. Unity-mode switched-capacitor converter to illustrate the basic operation.

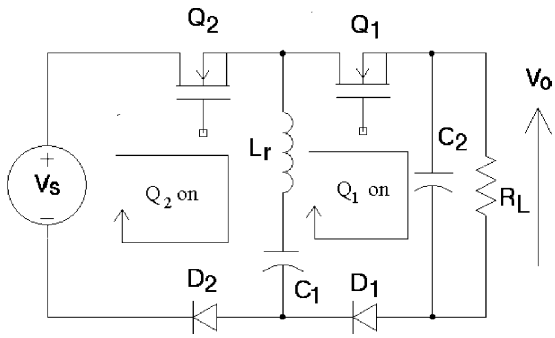

Fig. 2. Unity-mode switched-capacitor resonant converter.

[10] and [11]. This paper extends the concept and describes families of topologies of these circuitries and their generalized operation.

II. BASIC PRINCIPLE OF SWITCHED-CAPACITOR CONVERTER

The principle can first be explained by using a unity conversion ratio switched-capacitor converter. Fig. 1 shows the classical nonresonant switched-capacitor converter with unity conversion ratio. It can be seen that when Q_2 is turned on, C_1, the switching capacitor, is charged with the input voltage V_s. During this time D_2 is forward biased. When C_1 is fully charged to V_s, Q_2 is turned off and Q_1 is turned on. D_1 is forward biased and C_1 is, therefore, connected across the output. This classical version of the switched capacitor can be converted into a resonant version by inserting an inductor L_r in series with C_1 as shown in Fig. 2. Fig. 3 shows the corresponding waveforms. It can be seen that when Q_2 is turned on, L_r and C_1 start to resonate and zero current can be achieved. This current will resonate sinusoidally and return to zero after half of a resonance period. Because of the presence of diode D_2, the resonance stops naturally when the current i_{Lr} reaches zero. Therefore, the transistor is turned off under zero-current switching. Maximum energy is transferred from the source to C_1. The next stage is to turn on Q_1. Again, C_1 and L_r start to resonate in the loop as shown. The current also starts from zero and creates a zero-current turn-on.

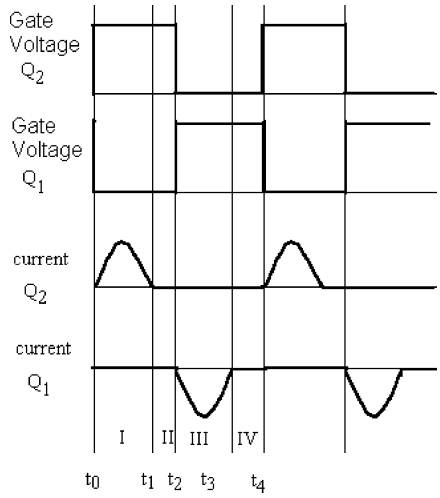

Fig. 3. Typical waveforms of the switched-capacitor converters.

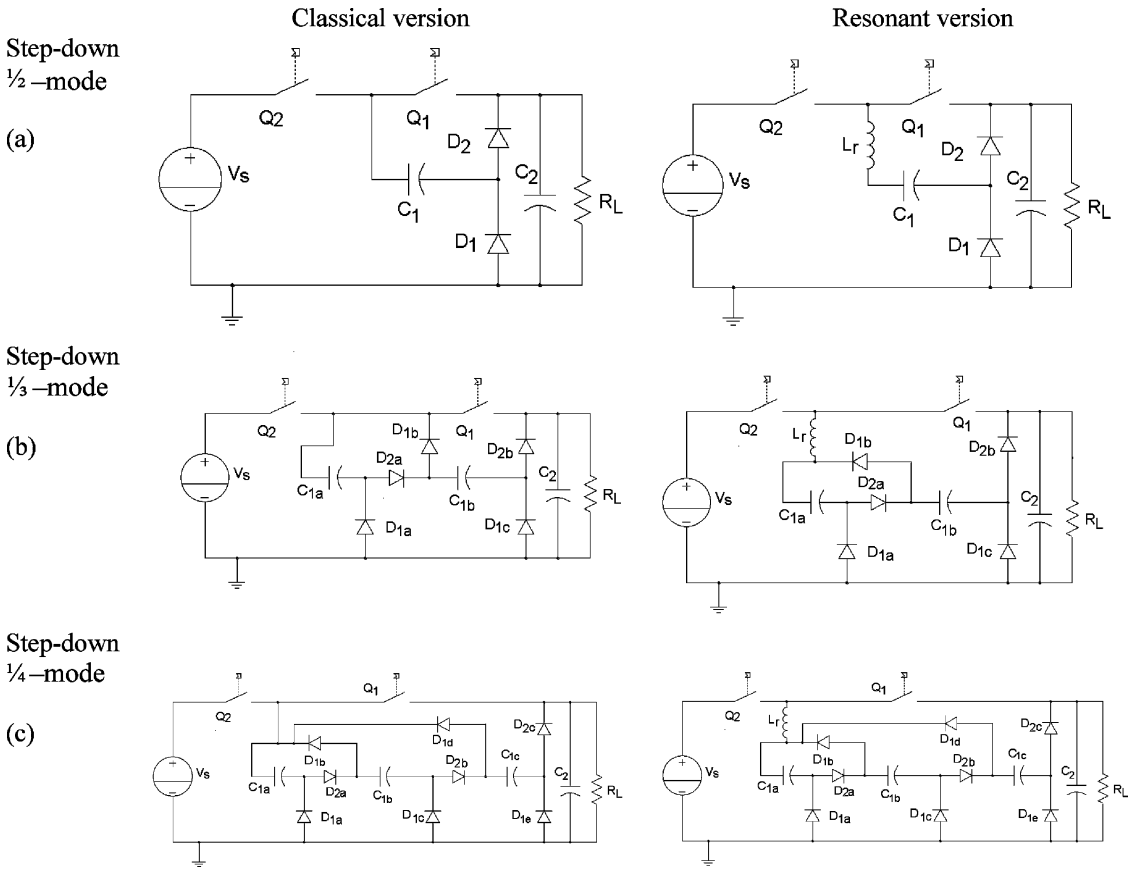

Fig. 4. Step-down converters.

C_1 is now transferring its energy back to the output. The resonant current also rises to a maximum value and then returns to zero after half a resonance period. The current stops naturally because of the presence of D_1. Zero-current turn-off can also be realized.

This principle shows that a classical switched-capacitor converter can now be transformed into a resonant version simply by inserting an inductor. By selecting the impedance and frequency of the resonant tank (C_1 and L_r), the peak value of the resonant current and the switching frequency can be controlled.

III. Families of the Switched-Capacitor Resonant Converter

The above principle has been applied to a series of the switched-capacitor converters. Fig. 4 shows the families of the step-down switched-capacitor resonant converter. The equivalent classical switched-capacitor converter is also shown as a comparison. Fig. 5 shows the step-up version of the family. Fig. 6 shows the inverting version of the converters. These versions represent three types of conversion ratios. Three topologies are shown for each family so that the reader can deduce the underlying mechanism to construct other conversion ratios.

In all three families, C_2 is usually large so that the output voltage can be assumed to be constant. L_r is a small inductor for creating resonance. It will resonate with other capacitors in various mesh loops when transistors Q_1 and Q_2 are turned on sequentially. It should also be noted that if L_r is removed from the circuit, the converter becomes the hard-switching classical switched-capacitor converter.

IV. Step-Down Circuits

A. Principle of Operation

Fig. 4(a)–(c) shows step-down circuits with voltage conversion ratios equal to 1/2, 1/3, and 1/4, respectively. It can be seen that these circuits basically consist of two transistors, Q_1 and Q_2, for routing to charge and discharge the switching capacitor C_1 [C_1 for Fig. 4(a), C_{1a}, C_{1b} for Fig. 4(b), C_{1a}, C_{1b}, C_{1c} for Fig. 4(c)]. The duty ratio of these transistors is usually 0.5 but the value is not critical. The operation of this concept can be explained by the 1/3-mode circuit as shown in Fig. 4(b). When Q_2 is turned on, C_{1a} and C_{1b} and L_r are connected in series resonance. D_{2a} and D_{2b} are forward biased. The resonance is designed in such a way that C_{1a} and C_{1b} contain a dc component, which is equal to $V_s/2$, and a small ac resonant component. The presence of L_r ensures that Q_2 is turned on under zero-current switching. After half a resonance cycle, the resonant current returns to zero and then is stopped by diodes D_{2a} and D_{2b}. Q_2 is, therefore, turned off under zero-current switching.

When Q_1 is next turned on, D_{2a} and D_{2b} are reverse biased and D_{1a}, D_{1b}, and D_{1c} are forward biased. C_{1a} and C_{1b} are connected in parallel, to produce series resonance together with L_r. This resonant tank is in parallel with C_2 through Q_1. Because C_2 is large, the resonance is mainly dependent on C_{1a}, C_{1b}, and L_r. Q_1 is also turned on and off under zero-current

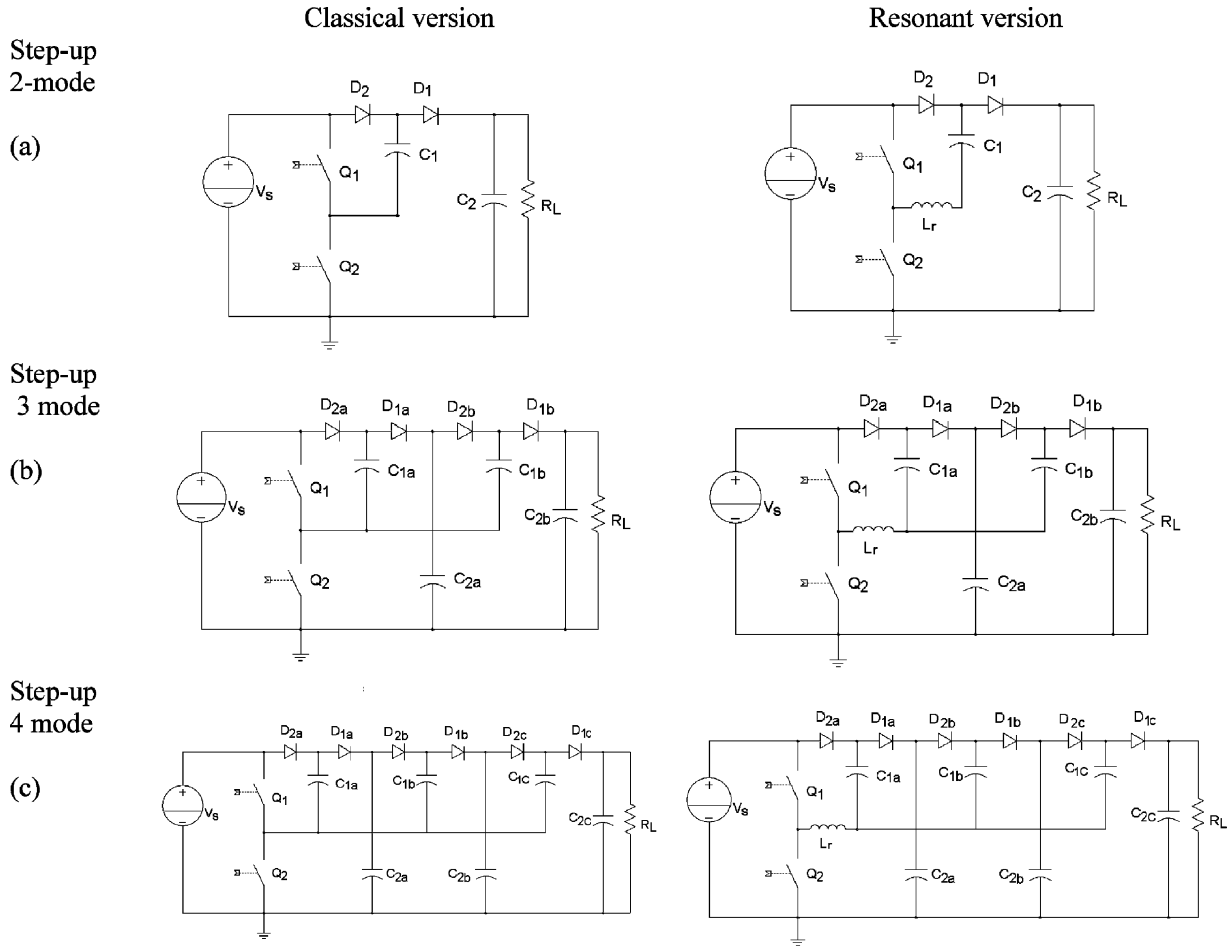

Fig. 5. Step-up converters.

switching in a way similar to that for Q_2 in the previous half-cycle. The voltage conversion ratio of the converter can be derived by balancing the input and output energy to be 1/3. The sizes of C_{1a}, C_{1b}, and C_2 are not necessarily equal. In practice, C_2 is much larger than C_{1a} and C_{1b}. The circuit components' states are summarized in Table II.

B. Equations of the Circuit

The equations of each state can be obtained by using the classical resonant circuit equation as shown in [11]. Also, one needs to equate the balance of the input and output energy and the continuity of the circuit voltage and current in order to obtain the coefficients of the equations. The equations of operation have been generalized as follows.:

For a $1/n$-mode circuit, one assumes that all the C_{1a}, $C_{1b}, \ldots$ are the same and each capacitor is represented by C_1. They are connected in parallel during States I and II and are in series during States III and IV. Let T_s be the period of the switching frequency, and i_L be the current of L_r. C_{1a}, C_{1b}, $C_{1c}, \ldots$ are connected in series and parallel in States I and III, respectively. When their capacitances are equal, their voltages are the same, hence, v_c is used to represent their voltage. Equations of the four states of operation can be derived and summarized as follows.

In State I $[t_0 - t_1]$,

$$v_C = V_0 - \frac{\pi I_0 T_S Z_0}{n(n-1)T_0} \cos\omega_0 (t - t_0) \tag{1}$$

$$i_L = \frac{\pi I_0 T_S}{nT_0} \sin\omega_0 (t - t_0) \tag{2}$$

where

$$\omega_0 = \sqrt{\frac{n-1}{L_r C_1}} = \frac{2\pi}{T_o} \tag{3}$$

$$Z_0 = \sqrt{\frac{(n-1)L_r}{C_1}}. \tag{4}$$

In State II $[t_1 - t_2]$,

$$v_C = V_0 + \frac{\pi I_0 T_S Z_0}{n(n-1)T_0} \tag{5}$$

$$i_L = 0. \tag{6}$$

In State III $[t_2 - t_3]$,

$$v_C = V_0 + \frac{(n-1)\pi I_0 T_S Z_1}{nT_1} \cos\omega_1 (t - t_2) \tag{7}$$

$$i_L = -\frac{(n-1)\pi I_0 T_S}{nT_1} \sin\omega_1 (t - t_2) \tag{8}$$

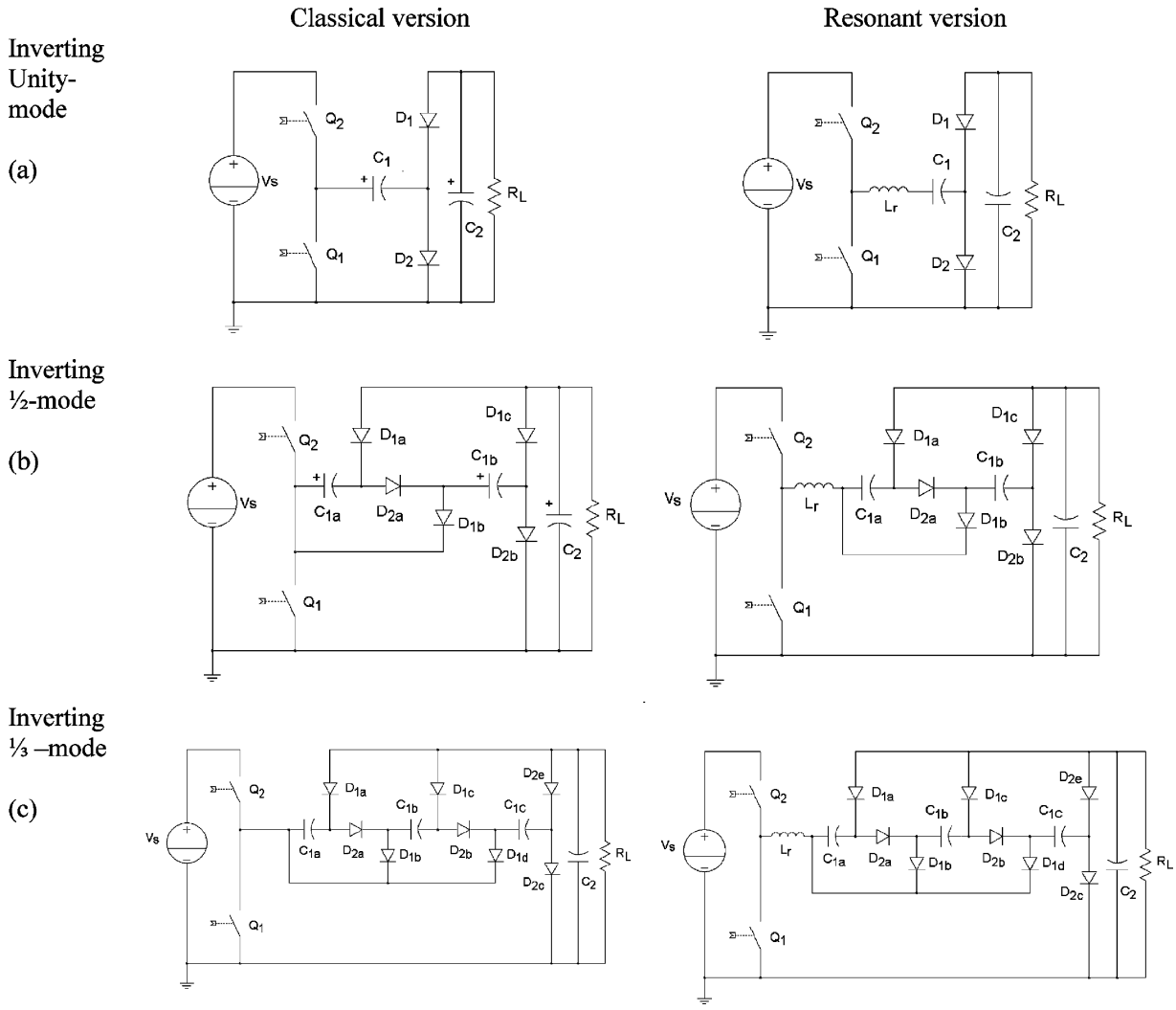

Fig. 6. Inverting converters.

TABLE II
SWITCHING DEVICES' STATES FOR THREE STEP-DOWN CIRCUITS

		Q_1 is on Q_2 is off	Q_2 is on Q_1 is off	Average Output voltage
½–mode	Diode states	D_1 = on	D_2 = on	½ V_s
	Average Voltage on C_1	½ V_s		
⅓–mode	Diode states	D_{1a}, D_{1b}, D_{1c} = on	D_{2a}, D_{2b}=on	⅓ V_s
	Average Voltage on C_{1a}, C_{1b}, C_{1c}	⅓Vs		
¼–mode	Diode states	D_{1a}, D_{1b}, D_{1c}, D_{1d}, D_{1e}=on	D_{2a}, D_{2b}, D_{2c} = on	¼ V_s
	Average voltage on C_{1a}, C_{1b}, C_{1c}	¼ V_s		

where

$$\omega_1 = \sqrt{\frac{1}{(n-1)\,L_r C_1}} \tag{9}$$

$$Z_1 = \sqrt{\frac{L_r}{(n-1)\,C_1}}. \tag{10}$$

In State IV $[t_3 - t_4]$,

$$v_C = V_0 - \frac{(n-1)\,\pi I_0 T_S Z_1}{nT_1} \tag{11}$$

$$i_L = 0. \tag{12}$$

TABLE III
SWITCHING DEVICES' STATES FOR THREE STEP-UP CIRCUITS

		Q_1 is on Q_2 is off	Q_2 is on Q_1 is off	Average output voltage
2–mode	Diode states	D_1 = on	D_2 = on	$2V_s$
	Average Voltage on C_1	V_s		
3–mode	Diode states	D_{1a}, D_{1b} = on	D_{2a}, D_{2b}=on	$3V_s$
	Average Voltage on C_{1a}, C_{1b}, C_{1c}	$C_{1a}=V_s$, $C_{1b}=2V_s$, $C_{1c}=2V_s$		
4–mode	Diode states	D_{1a}, D_{1b}, D_{1c}=on	D_{2a}, D_{2b}, D_{2c} = on	$4V_s$
	Average voltage on C_{1a}, C_{1b}, C_{1c}, C_{1d}, C_{1e}	$C_{1a}=V_s$, $C_{1b}=2V_s$, $C_{1c}=2V_s$, $C_{1d}=3V_s$, $C_{1e}=3V_s$		

V. STEP-UP CIRCUITS

A. Principle of Operation

Fig. 5(a)–(c) show the circuits with step-up ratio equal to 2, 3 and 4 respectively. The operation is very similar to that of the previous family. Q_1 and Q_2 are turned on and off alternatively. The operation is explained here by using the topology of Fig. 5(b). When Q_2 is turned on, D_{2a} and D_{2b} are forward biased. C_{1a} is in series resonance with L_r through D_{2a}. C_{1b} is also in series resonance with L_r through D_{2b} and C_{2a}. C_{1a} is charged by V_s, and C_{1b} is charged with a voltage equal to the voltage across C_{2a}. Usually, C_{2a} is larger than C_{1a} and C_{1b} so that its voltage is relatively constant.

When Q_1 is turned on in the second-half switching cycle, D_{2a} and D_{2b} are reverse biased. D_{1a} and D_{1b} are forward biased, hence, C_{1a} is connected in series with L_r and the source voltage to charge C_{2a}. C_{1b} is in series with L_r and source V_s to charge the output capacitor C_{2b}. Both Q_1 and Q_2 are turned on and off under zero-current switching in a manner similar to that of the step-down converters. The circuit components' states for each of the step-up circuits are summarized in Table III.

B. Equations of the Circuit

Similarly to the previous sections for States I and II, the capacitor C_{1a} is connected in series with L_r and the source V_s; C_{1b} is also connected in series with L_r and is driven by V_{c2a} which has an average value of $2V_s$. Therefore, the current through L_r also passes through all the resonant capacitors (C_{1a}, C_{1b}, ...).

During States III and IV, the capacitor C_1 is connected in series with L_r, the source, and C_{2a} which has an average voltage of $2V_s$. Similarly, C_{1b} is connected in series with L_r, the source, and C_{2b}, and so on. Now, then, the voltage across C_{1a}, C_{1b}, C_{1c}, ... is denoted by V_{Ci} where $i = a, b, c, \ldots$ Also, define $\varphi(i) = 1, 2, 3, 4 \ldots$ for $i = a, b, c, d, \ldots$, respectively. All the resonant capacitor currents also pass through L_r. Hence, for a $1/n$-mode, there are $n-1$ C_1 capacitors. Their equations can be described as follows.

In State I $[t_0 - t_1]$,

$$v_{C_i} = \varphi(i)V_s - \frac{n\pi I_0 T_S Z_o}{2T_0}\cos\omega_0(t - t_0) \tag{13}$$

$$i_L = \frac{n\pi I_0 T_S}{2T_0}\sin\omega_0(t - t_0) \tag{14}$$

where

$$\omega_0 = \sqrt{\frac{1}{L_r n C_1}} = \frac{2\pi}{T_o} \tag{15}$$

$$Z_0 = \sqrt{\frac{L_r}{nC_1}}. \tag{16}$$

In State II $[t_1 - t_2]$,

$$v_{C_i} = \varphi(i)V_s + \frac{n\pi I_0 T_S Z_0}{2T_0} \tag{17}$$

$$i_L = 0. \tag{18}$$

In State III $[t_2 - t_3]$,

$$v_C = \varphi(i)V_s + \frac{n\pi I_0 T_S Z_o}{2T_0}\cos\omega_o(t - t_2) \tag{19}$$

$$i_L = -\frac{n\pi I_0 T_S}{2T_0}\sin\omega_o(t - t_2). \tag{20}$$

In State IV $[t_3 - t_4]$,

$$v_C = \varphi(i)V_s - \frac{n\pi I_0 T_S Z_o}{2T_0} \tag{21}$$

$$i_L = 0. \tag{22}$$

VI. INVERTING CIRCUITS

A. Principle of Operation

Fig. 6 shows the family of inverting circuits. The operation of the circuit is explained by using Fig. 6(b). The operation is also very similar to that of the previous two families. Q_1 and Q_2 are turned on alternatively. When Q_2 is turned on, D_{2a} and D_{2b} are forward biased. C_{1a}, C_{1b}, and L_r are connected in series resonance with V_s. Because of the presence of L_r, the current through Q_2 is increased from zero in a resonating manner. Hence, Q_2 is under zero-current switching. After half a resonance cycle, the resonant current returns to zero but it cannot

TABLE IV
SWITCHING DEVICES' STATES FOR THREE INVERTING CIRCUITS

		Q_1 is on Q_2 is off	Q_2 is on Q_1 is off	Average output voltage
Unity–mode	Diode states	D_1 = on	D_2 = on	V_s
	Average Voltage on C_1	V_s		
½–mode	Diode states	D_{1a}, D_{1b}, D_{1c} = on	D_{2a}, D_{2b}=on	½ V_s
	Average Voltage on C_{1a}, C_{1b}, C_{1c}	C_{1a} =½V_s, C_{1b}=½V_s		
⅓–mode	Diode states	D_{1a}, D_{1b}, D_{1c}, D_{1d}, D_{1e} =on	D_{2a}, D_{2b}, D_{2c} = on	⅓ V_s
	Average voltage on C_{1a}, C_{1b}, C_{1c}, C_{1d}, C_{1e}	C_{1a}= ⅓V_s, C_{1b}=⅓V_s, C_{1c}=⅓V_s		

reverse because of the diodes D_{2a} and D_{2b} which stop the current from reversing. Therefore, Q_2 is turned off under zero-current switching.

When Q_1 is turned on in the next switching cycle, D_{1a}, D_{1b}, and D_{1c} are forward biased. C_{1a} and C_{1b} are connected in parallel and then in series resonance with L_r through Q_1. Similar zero-current switching operation occurs in Q_1. States of the circuit components of each of the step-up circuits are summarized in Table IV.

B. Equations of the Circuit

Similarly to the previous sections for States I and II, the capacitors C_{1a}, C_{1b}, ... are connected in series, and during States III and IV, the capacitors are connected in parallel. The voltage across C_1 capacitors can be assumed to be equal and denoted by V_c. Hence, for a $1/n$-mode converter in State I $[t_0 - t_1]$,

$$v_C = -V_0 + \frac{\pi I_0 T_S Z_0}{n^2 T_0} \cos\omega_0 (t - t_0) \tag{23}$$

$$i_L = -\frac{\pi I_0 T_S}{n T_0} \sin\omega_0 (t - t_0) \tag{24}$$

where

$$\omega_0 = \sqrt{\frac{n}{L_r C_1}} \tag{25}$$

$$Z_0 = \sqrt{\frac{n L_r}{C_1}}. \tag{26}$$

In State II $[t_1 - t_2]$,

$$v_C = -V_0 - \frac{\pi I_0 T_S Z_0}{n^2 T_0} \tag{27}$$

$$i_L = 0. \tag{28}$$

In State III $[t_2 - t_3]$,

$$v_C = -V_0 - \frac{\pi I_0 T_S Z_1}{T_1} \cos\omega_1 (t - t_2) \tag{29}$$

$$i_L = -\frac{\pi I_0 T_S Z_1}{T_1} \sin\omega_1 (t - t_2) \tag{30}$$

TABLE V
SPECIFICATIONS OF THE PROTOTYPE OF THE CONVERTERS

	Step-down	Step-up	Inverting
Mode	1/3	3	-1/2
Input voltage	90V	40V	60V
Output voltage	30V	120V	-30V
Output power	5W-80W	20W - 100W	10W - 70W
Switching frequency	200kHz	200kHz	200kHz
Q_1 and Q_2	IRF630	IRF530	IRF530
D_1 and D_2	MBR20100	MBR10100	MBR10100
C_{1a} and C_{1b}	0.22μF	0.22μF	0.22μF
C_{2a} and C_{2b} or C_2	50μF	100μF	100μF
L_r	1μH	1μH	1μH

where

$$\omega_1 = \sqrt{\frac{1}{n L_r C_1}} \tag{31}$$

$$Z_1 = \sqrt{\frac{L_r}{n C_1}}. \tag{32}$$

In State IV $[t_3 - t_4]$,

$$v_C = -V_0 + \frac{\pi I_0 T_S Z_1}{T_1} \tag{33}$$

$$i_L = 0. \tag{34}$$

VII. EXPERIMENTAL RESULTS

The three converter families have been constructed in order to verify their proposed operation. The experimental results of the 1/3-mode, 3-mode, and inverting 1/2-mode converters are shown here. The specifications of each of the prototype converters are listed in Table V.

The experimental waveforms of the three converters are shown in Figs. 7–9 for the step-down, step-up, and inverting circuits, respectively. The transistor's current is equal to the resonant inductor's current when the transistor is conducting. Examination of the amplitude and the frequency of the waveforms shows that they all agree with the theoretical findings as derived in (1)–(34). Fig. 10 shows efficiency and conversion ratio of each experiment. There is, however, a small reduction in the amplitude of the voltage by around 15% because of the resistive loss in the circuit. The dc output voltage is not exactly constant but is slightly dependent on the load, but that is a

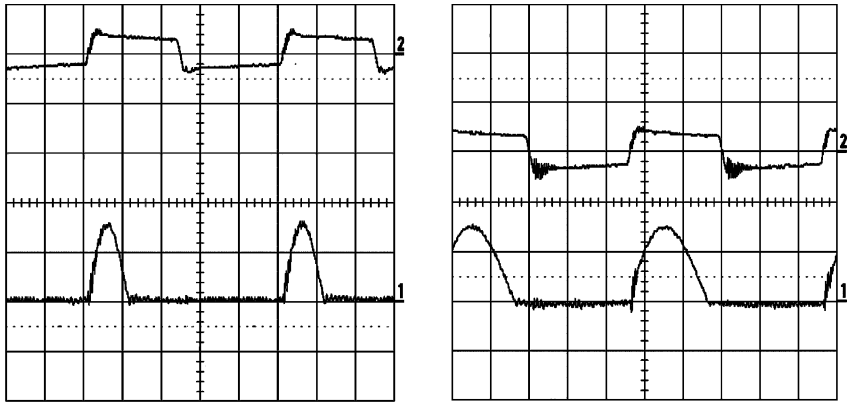

(a) Upper trace: Gate signal of Q_1, 40V/div
Lower trace: Drain current of Q_1, 5A/div

(b) Upper trace: Gate signal of Q_2, 40V/div
Lower trace: Drain current of Q_2, 5A/div

Fig. 7. Measured waveforms of the 1/3-mode switched-capacitor resonant step-down converter at 80 W.

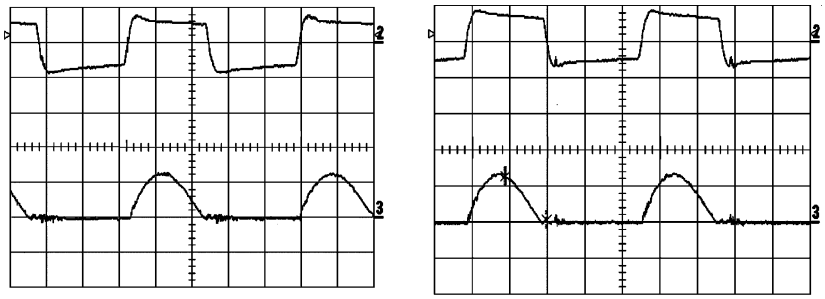

(a) Upper trace: Gate signal of Q_1, 20V/div
Lower trace: Drain current of Q_1, 5A/div

(b) Upper trace: Gate signal of Q_2, 20V/div
Lower trace: Drain current of Q_2, 5A/div

Fig. 8. Measured waveforms of the 3-mode switched-capacitor resonant step-up converter at 67 W.

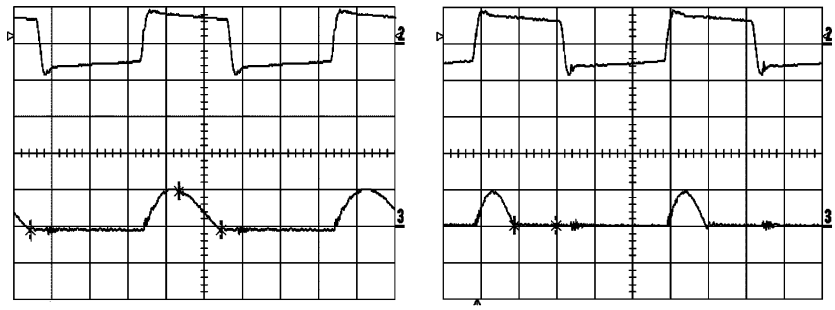

(a) Upper trace: Gate signal of Q_1, 40V/div
Lower trace: Drain current of Q_1, 5A/div

(b) Upper trace: Gate signal of Q_2, 40V/div
Lower trace: Drain current of Q_2, 5A/div

Fig. 9. Measured waveforms of the inverting 1/2-mode switched-capacitor resonant inverting converter at 52 W.

common feature for all the power converters. However, this dependence is small. Experimental results have shown that the output voltage varies by 10% only as the load varies by 400%. It can be seen that, for each case, the transistors Q_1 and Q_2 are both turned on and off under zero-current switching.

The efficiency has also been calculated by numerical estimation. The loss estimation is based on the classical method which is using the current passing through each of the components and corresponding resistance or on-state voltage drop. It can be seen that the theoretical prediction is very close to the measurement. It only deviated in the low-power region because the switching loss due to the parasitic capacitance of the switching devices, which is difficult to estimate accurately.

VIII. Comments

From the experimental results reported, it is clearly shown that zero-current switching has been achieved. All the transistors and diodes of all the topologies are switched on and off under zero-current switching. The diodes only allow unidirectional current to flow. This, therefore, forces the transistors to turn off naturally under zero-current switching. The principle

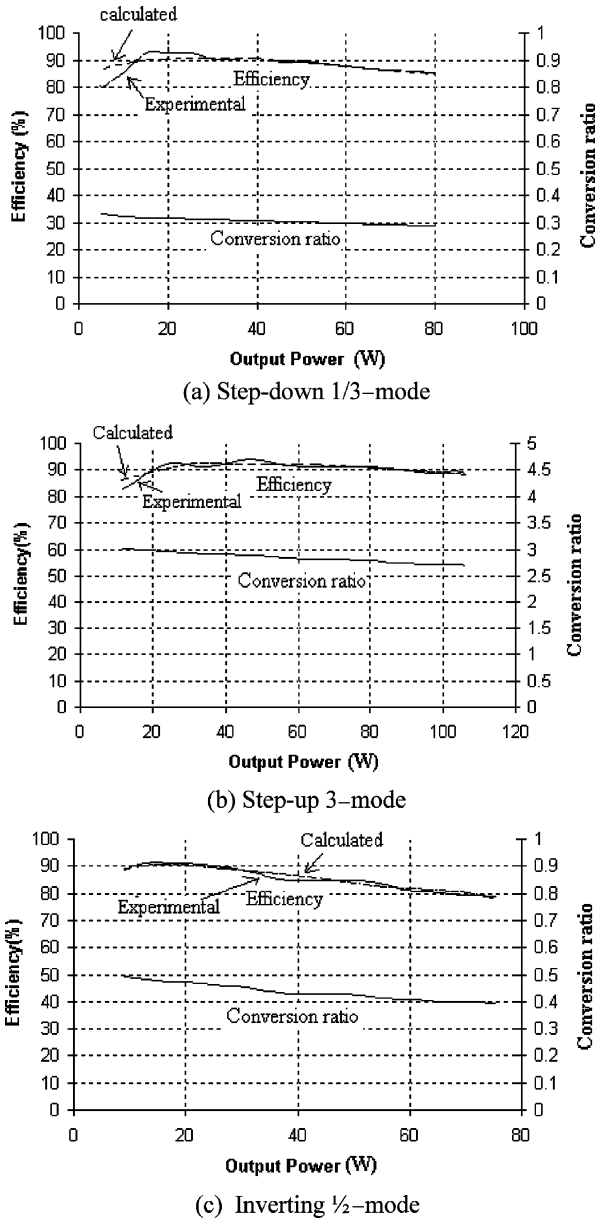

Fig. 10. Measured efficiencies and conversion ratios.

can be extended to other conversion ratios by simply adding capacitors and diodes. For example, by comparing Fig. 4(b) and (c), a conversion ratio of one-fourth can be obtained by adding an extra set of D_{2c}, D_{1e}, D_{1d}, and C_{1c} to Fig. 4(c). All the circuits have been validated by experiment and computer simulation, although computer simulation is not shown due to limited pages. The advantage of the circuits is that only two transistors are needed. High-power design is also possible because the zero-current switching has been used. The reduction in loss and EMI make the circuit become more practical. The disadvantage of these circuits is that the output voltage cannot be regulated by the duty ratio. The output voltage is fixed as was the previously mentioned dependent effect.

IX. Conclusion

A unified study of the switched-capacitor resonant converters has been presented. There are three converter families that can perform step-up, step-down, and inverting of the input voltage. Various conversion ratios can be produced by progressively adding additional switching capacitors and the associated diodes. Prototype converters have been constructed and tested. Experimental results show that the performance of these converters agrees well with the theoretical analysis. The efficiency of the proposed converters is high. The main contributions of the paper are as follows:

- propose a simple method to convert the classical switched-capacitor converter to have the zero-current switching feature;
- quantify the need of the inductor so that the switching current can be controlled, whereas the classical switched-capacitor has an uncontrolled spike current due to the parasitic inductance;
- produce families of converters with a wide range of numerical conversion ratios;
- produce theoretical analysis of the operation and their associated general circuit equations;
- experimental results for validating the operations.

References

[1] K. W. E. Cheng and P. D. Evans, "Parallel-mode extended-period quasiresonant converter," *Proc. Inst. Elect. Eng.*, pt. B, vol. 138, no. 5, pp. 243–251, Sept. 1991.

[2] ——, "Unified theory of extended-period quasiresonant converters," *Proc. IEE—Elect. Power Applicat.*, vol. 147, no. 2, pp. 119–130, Mar. 2000.

[3] H. Bengtsson, "A switch in methods," *New Electron.*, pp. 40–41, Aug 1997.

[4] O. C. Mak, Y. C. Wong, and A. Ioinovici, "Step-up DC power supply based on a switched-capacitor circuit," *IEEE Trans. Ind. Electron.*, vol. 42, pp. 90–97, Feb. 1995.

[5] J. Liu, Z. Chen, and Z. Du, "A new design of power supplies for pocket computer systems," *IEEE Trans. Ind. Electron.*, vol. 45, pp. 228–235, Apr. 1998.

[6] C. K. Tse, S. C. Wong, and M. H. L. Chow, "On lossless switched-capacitor power converter," *IEEE Trans. Power Electron.*, vol. 10, pp. 286–291, May 1995.

[7] M. S. Makowski and D. Maksimovic, "Performance limits of switched-capacitor DC-DC converters," in *Proc. IEEE PESC'95*, vol. 2, 1995, pp. 1215–1221.

[8] K. D. T. Ngo and R. Webster, "Steady-state analysis and design of a switched-capacitor DC-DC converter," *IEEE Trans. Aerosp. Electron. Syst.*, vol. 3, pp. 92–101, Jan. 1994.

[9] R. L. Steigerwald, "A comparison of half bridge resonant converter topologies," *IEEE Trans. Power Electron.*, vol. 3, pp. 174–182, Apr. 1988.

[10] K. W. E. Cheng, "New generation of switched capacitor converters," in *Proc. IEEE PESC'98*, 1998, pp. 1529–1535.

[11] ——, "Zero-current-switching switched-capacitor converters," *Proc. IEE—Elect. Power Applicat.*, vol. 148, no. 5, pp. 403–409, Sept. 2001.

Y. P. Benny Yeung was born in Hong Kong in 1974. He received the B.Eng. (Hons.) degree in electrical engineering in 1998 from The Hong Kong Polytechnic University, Hong Kong, where he is currently working toward the Ph.D. degree.

His principal research interests include soft switching of switched-mode power supplies and switched reluctance motor drives.

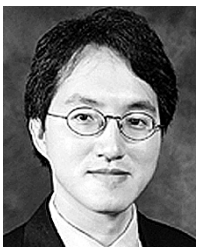

K. W. E. Cheng (M'90) received the B.Sc. and Ph.D. degrees from the University of Bath, Bath, U.K., in 1987 and 1990, respectively.

He was a Project Leader and Principal Engineer with Lucas Aerospace Ltd., U.K. In 1997, he joined The Hong Kong Polytechnic University, Hong Kong, where he is currently a Professor and Director of the Power Electronics Research Centre. His research involves all aspects of power electronics and drives. He has authored seven books and more than 150 papers published in international journals and conference proceedings.

Prof. Cheng received the IEE Sebastian Z. De Ferranti Premium Award for Best Paper in 1995, Outstanding Consultancy Award in 2000, and Merit Award of Best Teacher in 2003 from The Hong Kong Polytechnic University.

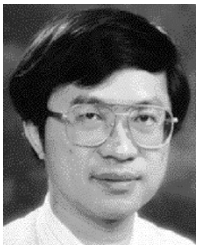

S. L. Ho received the B.Sc. (First Class Honors) and Ph.D. degrees from the University of Warwick, Warwick, U.K., in 1976 and 1979, respectively.

In 1979, he joined The Hong Kong Polytechnic University, Hong Kong, where he is currently a Professor in the Department of Electrical Engineering. His research interests are in the areas of traction engineering, finite-element analysis of electromagnetic devices, conditioning monitoring, and phantom loading of electrical machines. He has authored about 200 papers published in international journals and conference proceedings.

K. K. Law received the B.Eng. degree in electrical engineering from The Hong Kong Polytechnic University, Hong Kong, in 1999.

Following graduation, he became an Assistant Engineer with Chevalier (H.K. Ltd.). Since 2000, he has been a part-time Research Student at The Hong Kong Polytechnic University. His current research interests are switched-capacitor converters and power-factor correction.

Danny Sutanto (M'89–SM'94) received the B.Eng. and Ph.D. degrees from the University of Western Australia, Crawley, Australia, in 1978 and 1981, respectively.

Following graduation, he joined GEC Projects, Australia, as a Power System Analyst. In 1982, he joined the School of Electrical Engineering, University of New South Wales. Since 1996, he has been with The Hong Kong Polytechnic University, Hong Kong, where he is currently a Professor of Electrical Engineering. His main areas of research are power system analysis, power system economics, voltage stability, harmonics, power electronics, and computer-aided education.

Prof. Sutanto is currently the IEEE PES Region 10 Representative.